Tetrachloroethane (TeCA) removal through sequential graphite-mixed metal oxide electrodes in a bioelectrochemical reactor

Marco Zeppilli [a, *], Hafsa Yaqoubi [b], Edoardo Dell'Armi [a], Agnese Lai [a], Mustapha Belfaquir [b], Laura Lorini [a], Marco Petrangeli Papini [a]

[a] Department of Chemistry, University of Rome Sapienza, Piazzale Aldo Moro 5, Rome, 00185, Italy
[b] Department of Chemistry, Ibn Tofail University, Laboratory of Advanced Material and Process Engineering, Campus Universitaire, BP. 242, Kenitra, Morocco

ARTICLE INFO

ABSTRACT

Electro-bioremediation offers a promising approach for eliminating persistent pollutants from groundwater since allows the stimulation of biological dechlorinating activity, utilizing renewable electricity for process operation and avoiding the injection of chemicals into aquifers. In this study, a two-chamber microbial electrolysis cell has been utilized to achieve both reductive and oxidative degradation of tetrachloroethane (TeCA). By polarizing the graphite granules cathodic chamber at -650 mV vs the standard hydrogen electrode and employing a mixed metal oxide (MMO) counter electrode for oxygen production, the reductive and oxidative environment necessary for TeCA removal has been established. Continuous experiments were conducted using two feeding solutions: an optimized mineral medium for dechlorinating microorganisms, and synthetic groundwater containing sulphate and nitrate anions to investigate potential side reactions. The bioelectrochemical process efficiently reduced TeCA to a mixture of *trans*-dichloroethylene, vinyl chloride, and ethylene, which were subsequently oxidized in the anodic chamber with removal efficiencies of $37 \pm 2\%$, $100 \pm 4\%$, and $100 \pm 5\%$, respectively. The introduction of synthetic groundwater with nitrate and sulphate stimulated reductions in these ions in the cathodic chamber, leading to a 17% decrease in the reductive dechlorination rate and the appearance of other chlorinated by-products, including *cis*-dichloroethylene and 1,2-dichloroethane (1,2-DCA), in the cathode effluent. Notably, despite the lower reductive dechlorination rate during synthetic groundwater operation, aerobic dechlorinating microorganisms within the anodic chamber completely removed VC and 1,2-DCA. This study represents the first demonstration of a sequential reductive and oxidative bioelectrochemical process for TeCA mineralization in a synthetic solution simulating contaminated groundwater.

1. Introduction

Chlorinated aliphatic hydrocarbons (CAHs), such as tetrachloroethane (1,1,2,2-TeCA) and tetrachloroethene (PCE), are widespread groundwater contaminants often released as dense nonaqueous phase liquids (DNAPLs). These substances were widely used in industrial and civil applications due to their peculiar physico-chemical properties and low production costs. However, the massive production and utilization of chlorinated solvents have declined over the years due to environmental concerns stemming from improper storage or disposal [1]. In the United States alone, chlorinated solvents have been detected in 80% of contaminated groundwaters in superfund sites [2]. These contaminants, particularly their source zones, are challenging to remediate and represent a significant environmental liability. Over the past 30 years, the approach to remediating sites contaminated with chlorinated solvents has evolved. Initially, pump-and-treat systems were employed to contain and treat plumes and sources [3,4]. However, the focus has shifted towards more cost-effective plume treatment technologies, and more recently, *in situ* remediating sources [5,6]. Bioremediation technologies, which fall within the scope of "*in situ*" applications, are gaining the interest of specialists due to their cost-effective and flexible application. *In situ* bioremediation of groundwater involves encouraging indigenous bacterial

* Corresponding author.
E-mail address: marco.zeppilli@uniroma1.it (M. Zeppilli).

Abbreviation

CAHs	Chlorinated Aliphatic Hydrocarbons
TeCA	Tetrachloroethane
TCE	Trichloroethylene
TCA	Trichloroethane
DCA	Dichloroethane
cDCE	*cis*-Dichloroethylene
tDCE	*trans*-Dichloroethylene
VC	Vinyl Chloride
ETH	Ethylene
ETA	Ethane
RD	Reductive Dechlorination
SR	Sulphate reduction
NR	Nitrate Reduction
MMO	Mixed metal oxide

populations to metabolize target contaminants by adding an electron donor or acceptor. Indeed, high chlorinated contaminants, such as PCE or TeCA, can be reduced under anaerobic conditions by specialized dehalorespiring microorganisms using molecular hydrogen serves as an electron donor. This reaction, called reductive dechlorination (RD), successively replaces chlorine atoms with hydrogen atoms on the molecule carbon backbone, up to more acceptable and non-toxic molecules (i.e., ethylene). However, adverse environmental conditions, such as the lack of electron donor, can severely limit the complete dechlorination and lead to the accumulation of RD daughter products, such as dichloroethylene (DCE) or vinyl chloride (VC), which is the only carcinogen found [7,8].

In situ bioremediation occurred through direct metabolism, cometabolism, or abiotic transformations. Generally, for the high chlorinated CAHs, anaerobic degradation is the most appropriate process. In some conditions, anaerobic reductive bioremediation of PCE and trichloroethylene (TCE) may undergo incomplete degradation, leading to the formation of DCE or VC. This can occur due to factors such as the inability to achieve negative redox conditions or the lack of abundant *Dehalococcoides mccartyi*, the only known bacteria that can achieve the complete dechlorination of chlorinated ethenes [9]. However, less chlorinated compounds and dechlorination products, such as DCE, VC, and chloroethane, can be degraded using aerobic cometabolic or metabolic oxidative dechlorination pathways. As for cometabolic degradation, aerobic bacteria growing on hydrocarbons, such as methane or ethene, initiate their biodegradation by using dioxygenase or monooxygenase enzymes to convert these compounds into epoxides [10,11]. These oxygenases can fortuitously oxidize CAHs, yielding unstable chlorinated epoxides, which break down spontaneously into carbon monoxide, formate, glyoxylate, and chlorinated acids [12]. Several demonstration projects have transitioned to full-scale implementation, establishing reductive dechlorination as a widely accepted method for treating halogenated ethenes, ethanes, and methanes [13]. When designing an anaerobic reductive bioremediation system, key considerations include the competition of native electron acceptors (such as nitrate, iron, and iron sulphate) with the contaminant and the presence of bacteria capable of completely reducing contaminants [14]. Groundwater naturally contains various terminal electron acceptors that are utilized and depleted in a specific order based on their decreasing redox potential. In an anaerobic environment, nitrate is the first choice for electron acceptor [15]. An interesting approach studied in recent years involves the use of electrical stimulation of microbial

dechlorination in the presence of competing metabolisms, i.e., anions-reduction and methane-formation [16], promoting the complete denitrification in both reductive and oxidative environments [17,18]. Electrodes are used to manipulate the redox potential and to create favourable conditions for the RD [19], either through direct electron transfer from the electrodic surface to the dechlorinating microorganisms or via intermediate molecular hydrogen generation [20,21]. Furthermore, the less chlorinated CAHs were oxidized at the counter electrode through oxidative dechlorination (OD) stimulation via *in situ* oxygen evolution. In this frame, the combination of OD downstream to RD is an interesting option to implement full bioremediation of CAHs in contaminated groundwater [22,23]. The sequential reductive/oxidative bioelectrochemical process can be obtained in a single microbial electrolysis cell (MEC) equipped with an ion exchange membrane or by using two membrane-less reactors involving sacrificial graphite counterelectrodes [24]. Moreover, the degradation of TeCA remains largely unexplored, particularly in the presence of chloroethanes, chloroethenes, and other competing electron acceptors (e.g., nitrate and sulphate). Anaerobic biodegradation of TeCA can proceed either via dichloroelimination to form DCE, mediated by several dehalorespiring strains, or via hydrogenolysis to trichloroethane (TCA), for example, by *Dehalobacter* populations. Apparently, TeCA complete biodegradation requires dehalorespiring populations consortia. Additionally, a third mechanism known as dehydrochlorination, an abiotic non-redox process, can occur, resulting in the release of HCl and the formation of a double bond between two neighbouring carbon atoms. Hence, chloroethanes and chloroethenes can share common reaction intermediates (i.e., TCE, DCE, and VC), depending on chloroethane degradation pathways. For instance, DCE formation could result from both TeCA dichloroelimination and TCE hydrogenolysis. In this study, the focus was primarily on evaluating the pathways of TeCA transformation by a sequential cathodic and anodic bioelectrochemical reactor, which has previously been tested with other contaminants, such as TCE and Cr(VI) [25,26], in the absence and presence of competing reactions such as nitrate and sulphate reduction.

2. Materials and methods

2.1. Bioelectrochemical reactor setup

The bioelectrochemical reactor comprised identical cylindrical borosilicate glass chambers separated by a Nafion® 117 proton exchange membrane (PEM) Fig. 1. The cathode chamber was filled with graphite granules with diameters between 2 and 6 mm (El Carb 100, Graphite Sales, Inc, USA) as high-surface-area electrodes, and the external electrical connection was guaranteed by inserting graphite rod current collector (5 mm diameter, Sigma-Aldrich, Italy). The anodic electrodes were four Mixed Metal Oxides (MMOs; Magneto Special Anode, the Netherlands), with a projected
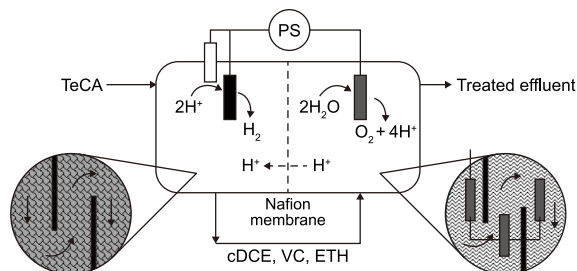

Fig. 1. Schematic representation of the experimental setup utilized during the study.

surface area of 8 cm^2 inserted into a bed of silica beads (size particles 2−5 mm). The electrical connection of the MMO anode to the potentiostat was ensured by a titanium wire (Sigma Aldrich, Italy). The total empty volume of the cathode and anode chambers were 0.82 and 0.95 L, respectively. An Ag/AgCl reference electrode (+0.2 V vs. standard hydrogen electrode, SHE; Amel, Milan, Italy) was placed in the cathode chamber. The cathode (working electrode), anode (counter electrode), and reference electrode were connected to a potentiostat Amel Model 549 (Milan, Italy). The reactor was equipped with three flow-through sampling cells (placed at the reactor inlet and the outlet of the cathode and the anode chambers, respectively). These cells were continuously and vigorously mixed with magnetic stirrers to promote the equilibrium between liquid (40 mL) and gaseous headspace (10 mL). Viton® tubes were utilized to minimize the adsorption of chlorinated compounds and volatilization losses. The mineral medium solution was constituted by an inorganic salt solution previously described [27], while the synthetic groundwater feeding solution was prepared by adding 55 mg L^{-1} NaNO$_3$ and 100 mg L^{-1} Na$_2$SO$_4$ to tap water. Both solutions have been contaminated with TeCA with a theoretical concentration of 50 μmol L^{-1}.

The reactor was continuously fed at a flow rate of 0.576 L d^{-1}, corresponding to an HRT of 1.42 and 1.65 d in the cathode and anode, and it was operated by controlling the cathode potential at −650 mV vs. SHE. The cathode and anode compartments were inoculated at the beginning of the experiment with specialized consortia capable of stably degrading CAHs by using hydrogen as an electron donor and oxygen as an electron acceptor. More specifically, the cathode chamber was inoculated with a TCE-to-ethene dechlorinating culture [28], previously enriched on hydrogen and TCE as an electron donor and acceptor. The bioelectrochemical reactor was operated at ambient temperature (25 ± 3 °C).

2.2. Tracer test set up

The step tracer test was performed by using a 0.02 M NaCl solution. Each reactor chamber, i.e., the anode and the cathode chamber, was characterized with an independent test. The step tracer test consisted of continuously feeding the tracer solution in the inlet of each chamber at a constant flow rate of 11.3 and 11.1 L d^{-1} for the anode and cathode tests, respectively. The test consisted of the continuous measure of the outlet liquid conductivity by a Handylab® 330 conductometer placed in each chamber's outlet. The conductivity (χ) continuously recorded was divided by the conductivity of the tracer's solution to obtain the F curve, which was used to determine the effective hydraulic retention time (HRT). The determination of the effective HRT allowed the calculation of the free volume in each chamber; moreover, the ratio between the effective and the geometric volume allowed the determination of the porosity of the reactor.

2.3. Analytical methods

The CAHs were determined by Dani GC 1000 (Contone, Switzerland) gas chromatograph equipped with a flame ionization detector (FID) using a header analyser HSS 86.50 (Dani, Contone, Switzerland). The gas chromatography analysis was conducted by a capillary TRB 264 column, 75 m of length, Teknokroma (Spain) (N$_2$ carrier gas: 18 mL min^{-1}; oven temperature: 80−210 °C; flame ionization detector temperature: 260 °C). Headspace concentrations were converted to aqueous-phase concentrations using tabulated Henry's law constants [29] and assuming equilibrium conditions between the gas and liquid phase. For all the chlorinated species, nominal concentrations were reported, representing the total amount (e.g., in moles) per unit of liquid volume. Methane,

hydrogen, and oxygen were measured in headspace samples using a DANI master gas chromatograph equipped with a thermal conductivity detector (TCD) (DANI Instruments, Contone, Switzerland). Liquid samples (1 mL) were taken using sterile disposable plastic syringes, filtered (0.22 μm), and analyzed for nitrate, nitrite, sulphate, and chloride, by using ion chromatography (0.5 mL sample, Dionex DX-100, Ionpac As9-Sc column, conductivity detector)

2.4. Calculations

The different biotic and abiotic TeCA dechlorination pathways are illustrated in Fig. 2. Three different mechanisms contribute to TeCA dichlorination: dichloroelimination, in which TeCA is biotically converted into cDCE; hydrogenolysis, a progressive reduction process resulting in the gradual loss of chlorine atoms; and dehydrochlorination, spontaneous abiotic degradation of saturated chlorinated compounds.

Each chlorinated species removal or production rate (μmol Ld^{-1}) was assessed by using the following equation:

$$\text{Removal or production rate} = \frac{[\text{CAHs}_{\text{out}}] - [\text{CAHs}_{\text{in}}]}{V_{\text{cathode}}} \times Q_{\text{out}} \qquad (1)$$

While the specific removal efficiency (%) of the target chlorinated species has been evaluated by the following equation:

$$\text{Removal efficiency }(\%) = \frac{[\text{CAHs}_{\text{in}}] - [\text{CAHs}_{\text{out}}]}{[\text{CAHs}_{\text{in}}]} \times 100 \qquad (2)$$

In equations (1) and (2), [CAHs$_{\text{in/out}}$] is the molar liquid concentration of the chlorinated compound.

The RD reaction rate (RD_{Rate}, μeq Ld^{-1}) in the presence of TeCA is calculated by taking into account only biological transformation mechanisms by the following equation:

where the CAH concentration is expressed as μmol L^{-1}, and V$_{\text{cathode}}$ represents the empty volume of the cathodic chamber of the
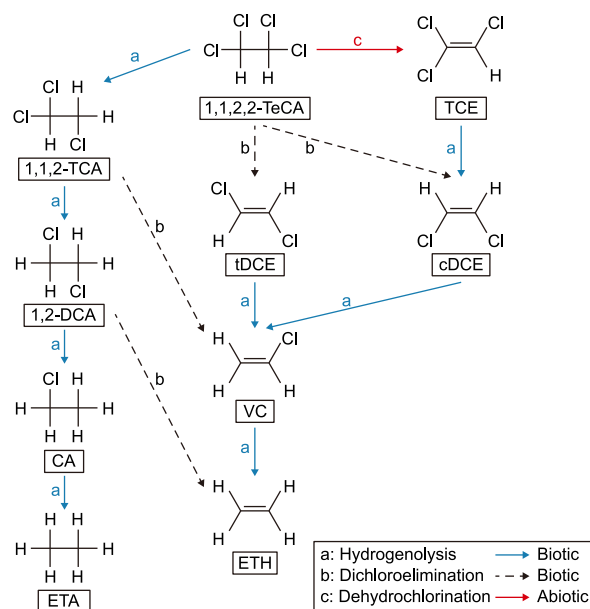

Fig. 2. Anaerobic degradation pathways for chloroethanes and chloroethenes. 1,1,2,2-TeCA: Tetrachloroethane; 1,1,2-TCA: Trichloroethane; 1,2-DCA: Dichloroethane; CA: Chloroethane; ETA: Ethane; TCE: Trichloroethene; DCE: Dichloroethene; VC: Vinyl chloride; ETH: Ethene. Modified from Ref. [29].

$$RD_{Rate} = \frac{[1,1,2-CA] \times 2 + [1,2-DCA] \times 4 + [cDCE] \times 2 + [tDCE] \times 2 + [VC] \times 4 + [ETH] \times 6 + [ETA] \times 8}{V_{cathode}} \times Q_{out} \tag{3}$$

bioelectrochemical reactor (0.86 L). The Coulombic efficiency for the reductive reactor (CE_{RD}, %) was calculated starting from the RD rate using the following equation:

$$CE_{RD} \ (\%) = \frac{RD_{Rate} \times \frac{F}{86400}}{I_{average}} \times 100 \tag{4}$$

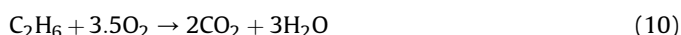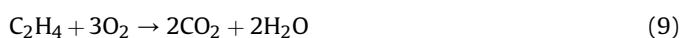where $I_{average}$ is the flowing current in the reductive reactor (mA), and F is Faraday's constant (96485 C mol^{-1}).

For the oxidative reactor, the oxidative dechlorination rate (OD, µmol Ld^{-1}) was calculated by the following equation:

$$\text{Oxidative dechlorination rate} = \frac{[C_{out}] - [C_{in}]}{V_{anode}} \times Q_{out} \tag{5}$$

while the oxidative removal efficiency (%) of each CAH (cDCE and VC) was calculated by the following equation:

$$\text{Oxidative removal efficiency} \ (\%) = \frac{[C_{in}] - [C_{out}]}{[C_{in}]} \times 100 \tag{6}$$

In the oxidative reactor, the oxidation rate for the chlorinated compounds was evaluated by considering the stoichiometry of cDCE and tDCE (equation (7)), VC (equation (8)), ethylene (ETH, equation (9)), and ethane (ETH, equation (10)) complete oxidation. 2, 2.5, 3, and 3.5 mol O$_2$ are required for the DCE, VC, ETH, and ETA complete oxidation, respectively.

$$C_2H_2Cl_2 + 2O_2 \rightarrow 2CO_2 + 2HCl \tag{7}$$

$$C_2H_3Cl + 2.5O_2 \rightarrow 2CO_2 + HCl \tag{8}$$

$$C_2H_4 + 3O_2 \rightarrow 2CO_2 + 2H_2O \tag{9}$$

$$C_2H_6 + 3.5O_2 \rightarrow 2CO_2 + 3H_2O \tag{10}$$

Moreover, considering the water oxidation reaction, four electrons are produced for each mole of oxygen, considering a complete conversion of the oxidation current into oxygen, the Coulombic efficiency for the oxidative reactor (CE_{OX}, %) can be expressed as

$$CE_{OX} \ (\%) = \frac{([cDCE_{removal}] \times 2 + [tDCE_{removal}] \times 2 + [VC_{removal}] \times 2.5 + [ETH_{removal}] \times 3 + [ETA_{removal}] \times 3.5) \times 4 \times \frac{F}{86400}}{[Average \ current]} \times 100 \tag{11}$$

Energy consumption of the process (kWh m^{-3}) was evaluated by considering the product of the average current (I) and the average cell voltage (ΔV) obtained during the reactor operation, according to the following expression:

$$\text{Energy consumption} = \frac{I \times \Delta V \times 24}{Q_{out}} \tag{12}$$

Calculations involved in side reactions and competitive mechanisms in the reductive reactor are reported in Table 1.

3. Results and discussion

3.1. Fluidynamic characterization of the bioelectrochemical reactor

The resulting F curve obtained for the two independent step curve tracer tests conducted in the cathodic and anodic chambers is shown in Fig. 3. From the evaluation of the F curve, two different HRTs were obtained for the anodic and cathodic chambers. Hence, two effective volumes were determined using a flow rate of 11.3 and 11.1 L d^{-1} for the anodic and cathodic chamber. As reported in Table 2, the effective anode chamber volume resulted in 0.4 L, while that of the cathode chamber was 0.58 L. Knowing the geometric volume of the two chambers, the porosity of each chamber was assessed, resulting in 0.7 for the cathode and 0.48 for the anode.

3.2. Performance of the bioelectrochemical process with the mineral medium solution

After the tracer test, the reactor was set in a continuous flow mode with an HRT of 1.42 d and fed with the mineral medium solution contaminated with TeCA. As reported in Fig. 4, the influent feeding solution showed an average TeCA concentration of 48 ± 3 µmol L^{-1}. Additionally, the influent solution contained an average TCE concentration of 2 ± 1 µmol L^{-1}. The TCE presence was a result of the spontaneous abiotic dehydrochlorination of the TeCA.

The main chlorinated by-products produced by the TeCA dechlorination are shown in Fig. 5a. During an initial transient period of approximately 45 days, the accumulation of VC, cDCE, and tDCE was observed. These by-products were generated through TeCA dichloroelimination and followed by the hydrogenolysis of the two DCE isomers. The RD reaction in the cathode compartment, utilizing a reductive potential of −650 mV vs. SHE, as shown in Fig. 6. Methanogenesis, which was the predominant side reaction during the first operational phase with the mineral medium, occurred concurrently with the RD process.

During the steady state condition, corresponding to days 50−120, the main RD by-products in the cathodic effluent were the tDCE, VC, and ETH with average concentrations of 3.7 ± 0.1, 18.7 ± 0.3 and 6.9 ± 0.3 µmol L^{-1}, respectively. Moreover, the only saturated by-product from TeCA reduction was ethane, which can

Table 1
The calculation for the competitive reactions in the cathode and anode chambers.

Reductive Reactor competitive mechanisms evaluation	
Sulphate (RD) removal rate (RS)	$RS\ (\mu eq\ Ld^{-1}) = \dfrac{Q_{liquid}}{V_{reductive}} \times [SO_4^{2-}]_{removed} \times 8$
	$RS\ (mA) = \dfrac{RS\ (\mu eq\ Ld^{-1}) \times V_{reductive} \times F}{86400}$
Nitrate (ND) removal rate (RN)	$RN\ (\mu eq\ Ld^{-1}) = \dfrac{Q_{liquid}}{V_{reductive}} \times [NO_3^{-}]_{removed} \times 5$
	$RN\ (mA) = \dfrac{RN\ (\mu eq\ Ld^{-1}) \times V_{reductive} \times F}{86400}$
Methane production rate $(RCH_{4(eq)})$	$RCH_4\ (\mu eq\ Ld^{-1}) = \dfrac{Q_{gas}}{V_{reductive}} \times [CH_4] \times 8$
	$RCH_4\ (mA) = \dfrac{RCH_4\ (\mu eq\ Ld^{-1}) \times V_{reductive} \times F}{86400 \times 1000}$
RS Coulombic efficiency (CE_{RS})	$CE_{RS}\ (\%) = \dfrac{RS\ (mA)}{I_{average}\ (mA)} \times 100$
RN Coulombic efficiency (CE_{RN})	$CE_{RS}\ (\%) = \dfrac{RN\ (mA)}{I_{average}\ (mA)} \times 100$
RCH_4 Coulombic efficiency (CE_{CH_4})	$CE_{CH_4}\ (\%) = \dfrac{RCH_4\ (mA)}{I_{average}\ (mA)} \times 100$

F: Faraday constant, 96485 C mol^{-1}; 86400: 86400 s per day; Q_{liquid}: Liquid flow rate; Q_{gas}: Gaseous flow rate.
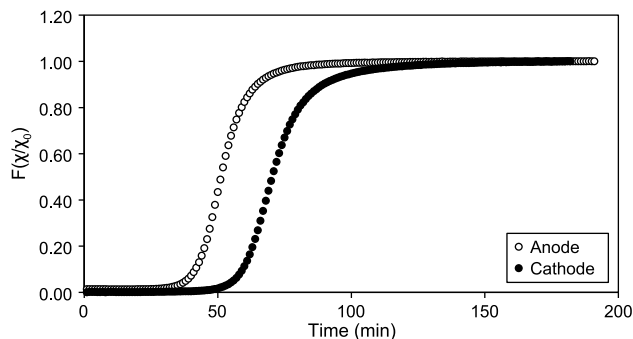

Fig. 3. F curves resulting from the anodic and cathodic tracer tests.

Table 2
Tracer test results for the anodic and cathodic chambers.

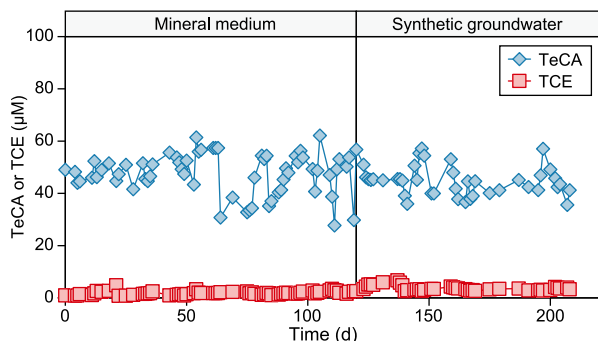| Parameters	Cathode	Anode
HRT (min)	73	52
Volume (L)	0.58	0.40
Porosity	0.70	0.42

Fig. 4. Time course of the feeding solutions CAH composition.

be produced by the hydrogenolysis of the ETH or by the hydrogenolysis of dichloroethane (DCA). As shown in Fig. 5b, ETA was present with an average concentration of $0.5 \pm 0.1\ \mu mol\ L^{-1}$. During
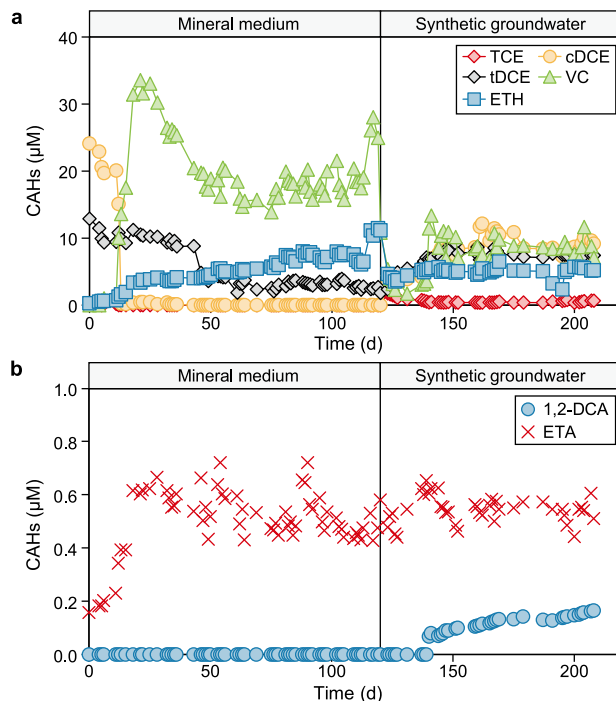

Fig. 5. Time course of the chlorinated ethenes (**a**) and ethanes (**b**) RD by-products in the cathodic effluent.

the first operating period, the VC emerged as the primary RD by-product, accounting for 63% of RD by-products and 38% of the influent TeCA. The VC predominance in the by-product composition was expected since the loss of the last chlorine from VC is considered the most challenging stage of the process. This reaction typically relies on the presence of specialized microorganisms, as it is generally cometabolic. In fact, many microorganisms can convert high-chlorinated compounds into lower-grade chlorination compounds, but only *Dehalococcoides mccartyi* can lead to a complete reduction to ethylene and only some microbial strains can draw energy from the reaction under examination. Furthermore, it is possible to hypothesize three different degradation pathways of TeCA that converge in the VC formation. The hydrogenolysis pathway, initiated by cDCE, and the dichloroelimination pathway, initiated by TCA, both contribute to the formation of VC. With reference to the latter reduction mechanism, all intermediates have a concentration below the detection limit of the instrument, however, the absence of TCA could derive from its quick reduction through both hydrogenolysis pathway and dichloroelimination with VC formation. Similarly, the absence of cDCE in the cathodic effluent indicates a quick reduction to VC through the hydrogenolysis mechanism, as reported in previous experiments and literature. Considering the different RD mechanisms, an average dechlorination rate of $61.6 \pm 0.4\ \mu eq\ Ld^{-1}$ was reached during the steady state operation of the cathodic chamber, which corresponded to an average Coulombic efficiency for the RD reaction of $2.6 \pm 0.3\%$ (Table 3). The Coulombic efficiency is a measure of the electric current utilized as the electron donor in the reductive dechlorination process. The main competitive reaction during the operating period with the mineral medium solution was methanogenesis, which usually occurred under anaerobic and electron donor-rich environments. The average methane production obtained during the first operating period reached $2295.1 \pm 0.6\ \mu eq\ Ld^{-1}$, corresponding to 7 mL Ld^{-1} with a Coulombic efficiency for the methane generation of $98.1 \pm 0.5\%$. Considering the two
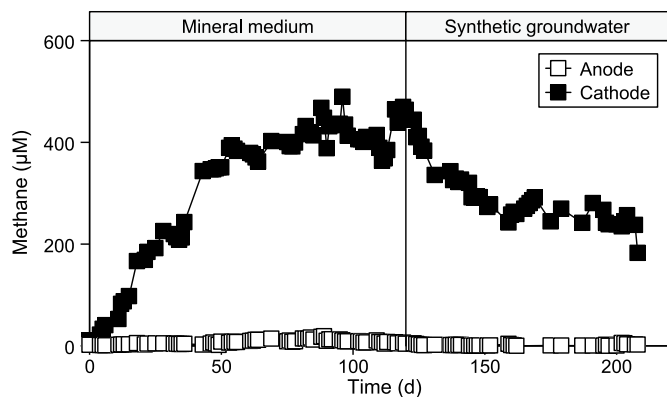
Fig. 6. Methane time course in the cathode and the anode outlet of the bioelectrochemical reactor.

Table 3
Coulombic efficiencies of the different reductive processes in the cathode chamber.

Reductive Coulombic efficiencies	Mineral medium	Synthetic groundwater
CE_{RD} (%)	2.6 ± 0.4	1.6 ± 0.3
CE_{CH_4} (%)	98.1 ± 0.5	51.1 ± 0.6
CE_{RS} (%)	-	14.5 ± 0.4
CE_{RN} (%)	-	31.9 ± 0.7
CE_{tot} (%)	100.7 ± 0.9	99.1 ± 2.0

reduction processes, a complete recovery of the current into reduced product was observed in the process, indicating a good description of the reaction mechanisms by the electron balance.

In the two-chamber bioelectrochemical reactor configuration, the effluent of the cathode chamber is the inlet solution for the

anodic reaction. Fig. 7 reports the detailed time course of the different RD by-products in the inlet and outlet of the anodic chamber. During the first operating period with the mineral medium solution, the anodic influent solution was mainly characterized by the presence of tDCE, VC, and ETH, whose profiles are described in detail in Fig. 7b, c, and 7d. As reported in each panel of Fig. 7, the oxidative environment produced by the electrolytic oxygen evolution (Fig. S1) sustained the complete biological oxidation of VC and ETH, while tDCE resulted in more recalcitrant, having an average concentration of 2.0 ± 0.2 μmol L^{-1} in the outlet. It is noteworthy to underline the capability of the aerobic dechlorinating microorganisms in the anodic chamber to oxidize more efficiently the VC than the tDCE due to the acclimatation strategy of the specialized aerobic inoculum adopted in the anodic chamber inoculation, which was acclimatized on ETH and cDCE [30,31]. Another important mechanism present in the anodic chamber of the bioelectrochemical reactor is the oxidation of the influent CH_4 by specialized microorganisms already shown in Fig. 6. Considering the whole oxidative processes in the anode chamber, i.e., the oxidation of each RD by-product, the oxygen evolution (Fig. S1), and the methane oxidation, the Coulombic efficiency for the oxidative processes was 8.4 ± 0.7%, 59.3 ± 0.8%, and 95.7 ± 0.5% (Table 3), respectively. The overall Coulombic efficiency for the oxidative processes, considerably higher than 100%, was probably affected by the overestimation of the methane production, which was assessed considering the liquid concentration and flow rate of the reactor.

3.3. Performance of the bioelectrochemical process with the synthetic groundwater

Starting from day 120, the feeding solution was substituted by synthetic groundwater consisting of tap water added with nitrate
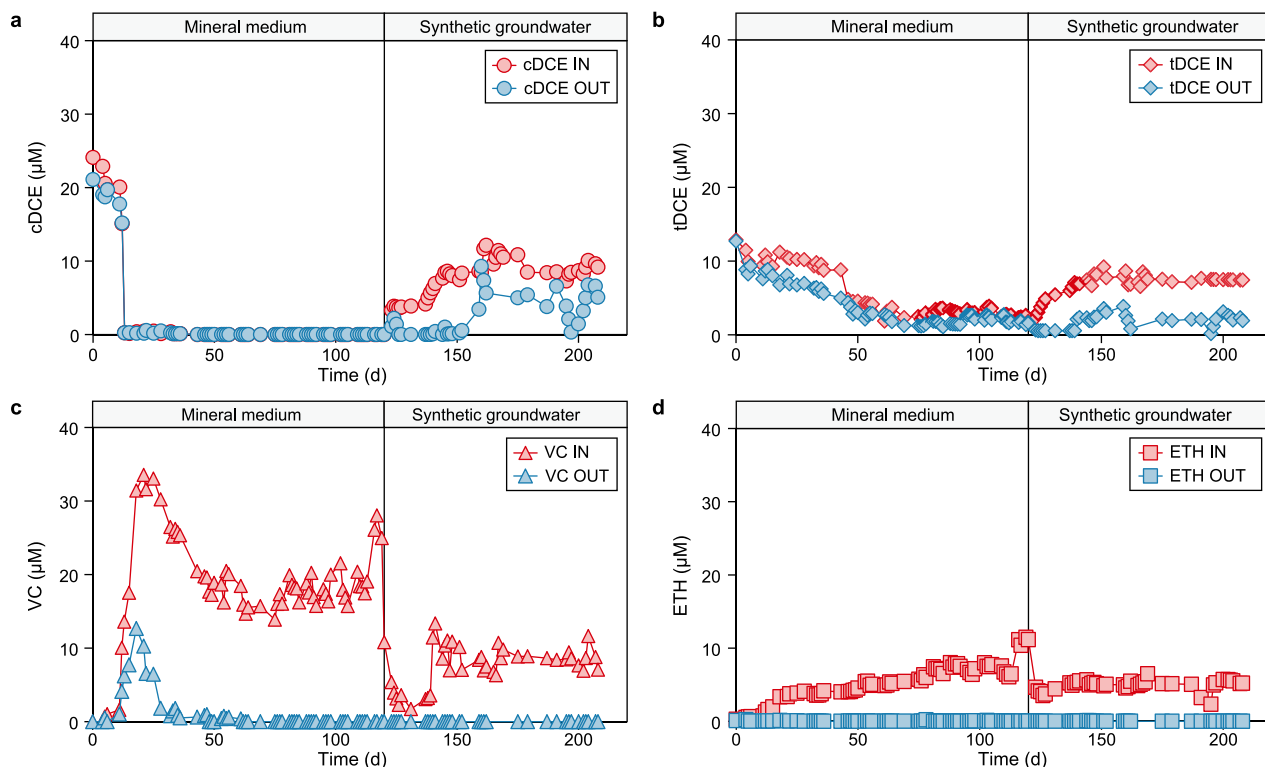

Fig. 7. Time course of the inlet and outlet cDCE (**a**), tDCE (**b**), VC (**c**), and ETH (**d**) in the oxidative reactor.

and sulphate anions [16]. Following the same procedure for the feeding solution contamination with TeCA, as shown in Fig. 3, a stable concentration of 45.0 ± 0.5 mol L^{-1} of TeCA was fed to the bioelectrochemical reactor; moreover, an average concentration of 2.4 ± 0.3 μmol L^{-1} of TCE was detected in the feeding solution, due to the partial abiotic degradation of TeCA through the dehydrochlorination mechanism.

The change of the contaminated feeding solution promoted a transient period of about 15 days, which finished around day 140. Then the new steady-state operating period was characterized by a complete TeCA removal through the cathodic chamber. As already observed in a previous study [32], the insertion of the synthetic groundwater promoted the variation of the RD by-products spectra, indeed, as reported in Fig. 5a, the concentrations of cDCE and tDCE progressively increased over time up to an average concentration of 9.0 ± 0.4 and 7.5 ± 0.2 μmol L^{-1}, respectively. On the other hand, VC concentration decreased by about 50% compared to feeding with mineral medium, from 18.7 ± 0.3 to 8.9 ± 0.5 μmol L^{-1}. On the contrary, ETH was less affected by the feeding solution shift, with a small concentration decrease from 6.9 ± 0.3 to 5.0 ± 0.3 μmol L^{-1}. The RD rate decreased to 51.1 ± 0.2 μeq Ld^{-1}, a 17% lower value with respect to the previous mineral medium operation. Like the RD, the methane concentration (Fig. 6) decreased until reaching an average liquid concentration of 267 ± 6 μmol L^{-1}, about 35% lower than the synthetic medium. This partial inhibition of the RD and methanogenesis reactions was probably induced by competing metabolisms for the available reducing power in the cathodic chamber. Indeed, the synthetic groundwater contains nitrate and sulphate, which represent antagonistic and preferred electron acceptors of the microbial consortium, competing with dechlorinating microorganisms for the hydrogen produced and the electrons supplied within the cathode compartment. As reported in Fig. 8a, nitrate was completely reduced in the cathodic chamber, while the sulphate ion was only partially removed.

Considering a 98% and 18% removal efficiency of the nitrate and sulphate ions within the cathodic chamber, an average removal rate of 17.3 ± 0.1 and 8.6 ± 0.3 mg Ld^{-1} was observed. Considering the whole reductive processes active in the cathodic chamber of the electrochemical reactor [i.e., RD, methanogenesis, nitrate reduction (RD), sulphate reduction (SR)], the corresponding Coulombic efficiency was $1.6 \pm 0.1\%$ for the RD reaction, $45.8 \pm 0.3\%$ for the methanogenesis, $30.0 \pm 0.5\%$ and $15.3 \pm 0.4\%$ for the NR and SR reactions. An overall current recovery of 92.8% was obtained considering the four different electron-consuming mechanisms, as reported in Table 4 and represented in Fig. 9.

The effect of introducing the synthetic groundwater solution in the oxidative side of the bioelectrochemical reactor, i.e., the anodic chamber of the reactor, which constituted the counterelectrode part of the cell, is reported in Fig. 7, in which all RD by-product oxidations are reported. After the introduction of the synthetic groundwater solution, the oxidation capacity of the anode on VC and ETH, reported respectively in Fig. 7c and d, was not affected, i.e., the removal efficiency of the VC and ETH resulted complete with a corresponding removal rate of 6.3 ± 0.1 and 3.6 ± 0.3 μmol Ld^{-1}. On the other hand, the cDCE concentration increase in the cathode effluent, after the insertion of the synthetic groundwater media, led only to a partial oxidation of the cDCE (removal efficiency $64 \pm 2\%$) while the tDCE removal efficiency increased from $37 \pm 2\%$ to $71 \pm 4\%$. Moreover, as reported in Figs. S2 and S3, a nearly complete oxidation of residual DCA and ETA was obtained in the anode chamber. Table 5 reports the removal rates and the corresponding removal efficiencies for each chlorinated aliphatic hydrocarbon oxidized in the anodic chamber of the reactor during the two operating periods.
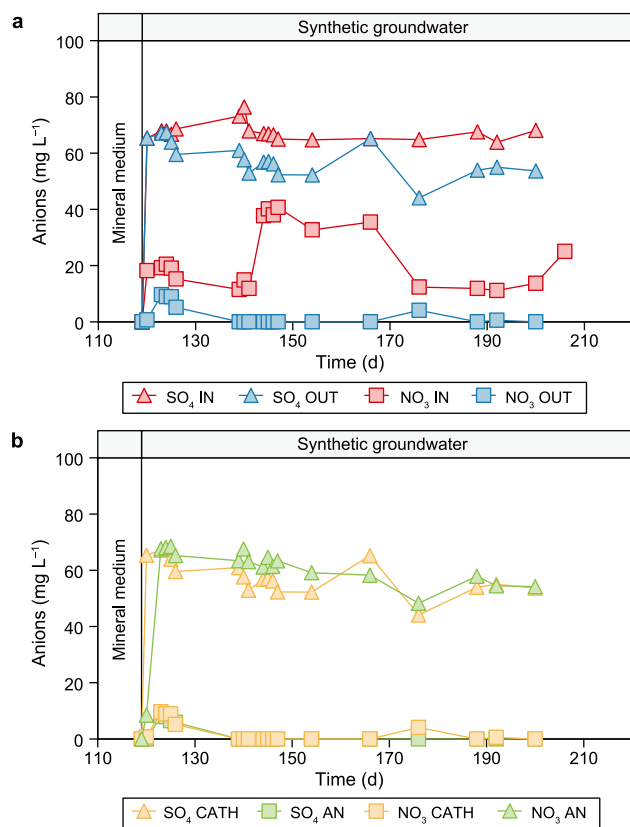
3.4. Energetic consumption of the process

The energy consumption of the bioelectrochemical reactor was simply assessed by considering the average current and cell voltage

Table 4
Electron recovery expressed as Coulombic efficiency in the anodic chamber.

Reductive Coulombic efficiencies	Mineral medium	Synthetic groundwater
$CE_{OD(CAHs)}$ (%)	2.6 ± 0.4	1.6 ± 0.3
$CE_{OD(CH_4)}$ (%)	98.1 ± 0.5	51.1 ± 0.6
CE_{O_2} (%)	59 ± 0.8	48 ± 1.1

Fig. 8. Time course of nitrate and sulphate concentration in the cathodic (**a**) and anodic (**b**) chamber of the bioelectrochemical reactor.
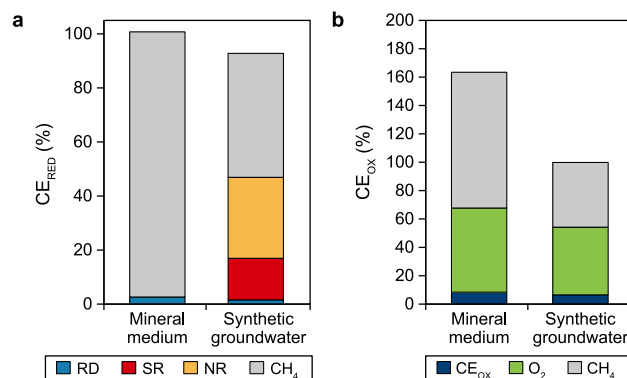

Fig. 9. Electron balance of the reductive (**a**) and oxidative (**b**) processes in the bioelectrochemical reactor.

Table 5
CAH oxidation capacity expressed as removal rates and removal efficiencies during the two operating periods.

Compound	Mineral medium		Synthetic groundwater	
	Removal rate (μmol Ld^{-1})	Removal efficiency (%)	Removal rate (μmol Ld^{-1})	Removal efficiency (%)
TCE	-	-	4.9 ± 0.2	94 ± 1
cDCE	-	-	4.9 ± 0.1	64 ± 2
tDCE	0.8 ± 0.2	37 ± 2	3.7 ± 0.2	71 ± 4
DCA	-	-	4.9 ± 0.1	94 ± 6
VC	12.9 ± 0.3	100 ± 4	6.3 ± 0.1	100 ± 5
ETH	4.8 ± 0.4	100 ± 5	3.6 ± 0.3	100 ± 4
ETA	0.3 ± 0.1	100 ± 3	0.4 ± 0.1	99 ± 2

Table 6
Energetic consumption of the process during the two operating periods.

Parameters	Mineral medium	Synthetic groundwater
I (mA)	-2.14 ± 0.13	-3.0 ± 0.21
ΔV (V)	-2.19 ± 0.22	-2.33 ± 0.31
$E_{counter}$ (V)	1.54 ± 0.11	1.71 ± 0.20
Energy consumption (kWh m^{-3})	0.20 ± 0.06	0.29 ± 0.08

established during the potentiostatic polarization of the system at -650 mV vs. SHE. During the first operating period, when the mineral medium was used as liquid media, the average current was -2.14 ± 0.13 mA (Fig. S4). To maintain the desired cathodic potential, the potentiostat applied -2.19 ± 0.22 V between the cathode and anode, resulting in an average counterelectrode potential of $+1.54 \pm 0.11$ V vs. SHE. During the operation of the bio-electrochemical process with synthetic groundwater, the average current and cell voltage were measured at -3.0 ± 0.21 mA and -2.33 ± 0.31 V (Fig. S4), resulting in a counterelectrode potential of $+1.71 \pm 0.20$ V vs. SHE. Considering continuous reactor operation for 24 h and the treated liquid flow in both runs (0.576 L), the energy consumption of the process was calculated to be 0.20 ± 0.06 and 0.29 ± 0.08 kWh m^{-3} of the treated solution (Table 6). The energy consumption of the process was extremely contained and consistent with similar approaches documented in the literature [17,33].

4. Conclusions

This study presents a pioneering investigation into the degradation pathways of TeCA in a sequential cathode-anode bio-electrochemical reactor fed with a mineral medium and synthetic groundwater. TeCA was degraded by the cathodic dechlorinating biofilm via multiple reaction pathways, including hydrogenolysis and dichloroelimination. The target contaminant was reduced by about 99% into DCEs and VC and in small quantities in ETH. Apparently, the relative importance of chlorinated ethene hydrogenolysis, with respect to dichloroelimination, increased as the chlorination degree decreased. TeCA degradation occurred mostly through dichloroelimination, which resulted in a peak concentration of overall DCEs (both the *cis-* and *trans-*isomers), comprising up to 30% of initial TeCA. Additionally, a minor extent of degradation was observed through hydrogenolysis, leading to the formation of DCA. The TCA produced from the hydrogenolysis of TeCA was not present in cathodic effluent at a steady state.

The introduction of sulphate and nitrate into the feeding solution composition led to a decrease in the reductive dechlorination rate. This decrease can be attributed to the occurrence of side reactions, such as NR and SR. Therefore, the RD reaction rate was slightly decreased, as confirmed by increased cDCE concentration in the cathodic effluent. The Coulombic efficiency of the RD reaction resulted lowered from 2.6% to 1.5% in the presence of NR and SR

side reactions.

The nitrate reduction process was rapid and nearly complete, while the reverse was true for sulphate anion degradation, which only occurred to a minor extent (13%). As expected, depleting the sulphate from the groundwater may not be necessary to achieve substantial dechlorination.

Previous studies indicated that reductive dechlorination was inhibited by the competition for available electron donors in the presence of nitrate or sulphate. Indeed, the Coulombic efficiency showed that most of the current was used by competitive reactions, especially nitrate reduction, while the reductive dechlorination process accounted for only 2% of the current. Overall, the oxidative reactions in the anode compartment allowed for consistent removal of saturated and unsaturated RD by-products, especially the VC, which usually represents the bottleneck of *in situ* remediation.

CRediT authorship contribution statement

Marco Zeppilli: Investigation, Writing - Original Draft, Funding Acquisition. **Hafsa Yaqoubi:** Investigation. **Edoardo Dell'Armi:** Investigation, Writing - Original Draft. **Agnese Lai:** Investigation. **Mustapha Belfaqui:** Supervision. **Laura Lorini:** Writing - Review & Editing. **Marco Petrangeli Papini:** Supervision.

Declaration of competing interest

The authors declare that they have no known competing financial interests or personal relationships that could have appeared to influence the work reported in this paper.

Acknowledgements

Appendix A. Supplementary data

Supplementary data to this article can be found online at https://doi.org/10.1016/j.ese.2023.100309.

References

[1] P.L. McCarty, Groundwater Contamination by Chlorinated Solvents: History, Remediation Technologies and Strategies, 2010, pp. 1–28, https://doi.org/10.1007/978-1-4419-1401-9_1.

[2] USEPA (U.S. Environmental Protection Agency), Cleaning up the Nation's Waste Sites: Markets and Technology Trends, 2004.

[3] A. Casasso, T. Tosco, C. Bianco, A. Bucci, R. Sethi, How Can We Make Pump and Treat Systems More Energetically Sustainable?, Water (Switzerland), 2020, p. 12, https://doi.org/10.3390/w12010067.

[4] D.M. Mackay, J.A. Cherry, Groundwater Contamination: Pump-And-Treat

Remediation, 1989, p. 23.

[5] P. Ciampi, C. Esposito, E. Bartsch, E.J. Alesi, G. Rehner, M. Petrangeli Papini, Remediation of chlorinated aliphatic hydrocarbons (CAHs) contaminated site coupling groundwater recirculation well (IEG-GCW®) with a peripheral injection of soluble nutrient supplement (IEG-C-MIX) via multilevel-injection wells (IEG-MIW), Heliyon 11 (2022), https://doi.org/10.1016/j.heliyon.2022.e11402.

[6] M. Majone, R. Verdini, F. Aulenta, S. Rossetti, V. Tandoi, N. Kalogerakis, S. Agathos, S. Puig, G. Zanaroli, F. Fava, In situ groundwater and sediment bioremediation: barriers and perspectives at European contaminated sites, N. Biotech. 32 (2015) 133−146, https://doi.org/10.1016/j.nbt.2014.02.011.

[7] F. Aulenta, A. Catervi, M. Majone, S. Panero, P. Reale, S. Rossetti, Electron transfer from a solid-state electrode assisted by methyl viologen sustains efficient microbial reductive dechlorination of TCE, Environ. Sci. Technol. 41 (2007) 2554−2559, https://doi.org/10.1021/es0624321.

[8] M.M. Rossi, E. Dell'Armi, L. Lorini, N. Amanat, M. Zeppilli, M. Villano, M. Petrangeli Papini, Combined strategies to prompt the biological reduction of chlorinated aliphatic hydrocarbons : new sustainable options for bioremediation application, Bioengineering 8 (2021) 109, https://doi.org/10.3390/bioengineering8080109.

[9] F.E. Löffler, J. Yan, K.M. Ritalahti, L. Adrian, E.A. Edwards, K.T. Konstantinidis, J.A. Müller, H. Fullerton, S.H. Zinder, A.M. Spormann, Dehalococcoides mccartyi gen. nov., sp. nov., obligately organohalide-respiring anaerobic bacteria relevant to halogen cycling and bioremediation, belong to a novel bacterial class, Dehalococcoidia classis nov., order Dehalococcoidales ord. nov. and family Dehalococcoidaceae fam. nov., within the phylum Chloroflexi, Int. J. Syst. Evol. Microbiol. 63 (2013) 625−635, https://doi.org/10.1099/ijs.0.034926-0.

[10] T.E. Mattes, A.K. Alexander, N.V. Coleman, Aerobic biodegradation of the chloroethenes: pathways, enzymes, ecology, and evolution, FEMS Microbiol. Rev. 34 (2010) 445−475, https://doi.org/10.1111/j.1574-6976.2010.00210.x.

[11] S.T. Lohner, D. Becker, K.M. Mangold, A. Tiehm, Sequential reductive and oxidative biodegradation of chloroethenes stimulated in a coupled bioelectroprocess, Environ. Sci. Technol. 45 (2011) 6491−6497, https://doi.org/10.1021/es200801r.

[12] P. Pant, S. Pant, A review: advances in microbial remediation of trichloroethylene (TCE), J. Environ. Sci. 22 (2010) 116−126, https://doi.org/10.1016/S1001-0742(09)60082-6.

[13] H.F. Stroo, A. Leeson, J.A. Marqusee, P.C. Johnson, C.H. Ward, M.C. Kavanaugh, T.C. Sale, C.J. Newell, K.D. Pennell, C.A. Lebrón, M. Unger, Chlorinated ethene source remediation: lessons learned, Environ. Sci. Technol. 46 (2012) 6438−6447, https://doi.org/10.1021/es204714w.

[14] F. Aulenta, M. Beccari, M. Majone, M.P. Papini, V. Tandoi, Competition for H2 between sulfate reduction and dechlorination in butyrate-fed anaerobic cultures, Process Biochem. 43 (2008) 161−168, https://doi.org/10.1016/j.procbio.2007.11.006.

[15] F.E. Löffler, J.M. Tiedje, R.A. Sanford, Fraction of electrons consumed in electron acceptor reduction and hydrogen thresholds as indicators of halorespiratory physiology, Appl. Environ. Microbiol. 65 (1999) 4049−4056, https://doi.org/10.1128/aem.65.9.4049-4056.1999.

[16] M. Tucci, C.V. Carolina, M. Resitano, B. Matturro, S. Crognale, I. Pietrini, S. Rossetti, F. Harnisch, F. Aulenta, Simultaneous removal of hydrocarbons and sulfate from groundwater using a "bioelectric well", Electrochim. Acta 388 (2021) 138636 https://doi.org/10.1016/J.ELECTACTA.2021.138636.

[17] E. Dell'Armi, M. Zeppilli, F. De Santis, M. Petrangeli Papini, M. Majone, Control of sulfate and nitrate reduction by setting hydraulic retention time and applied potential on a membraneless microbial electrolysis cell for perchloroethylene removal, ACS Omega (2021), https://doi.org/10.1021/acsomega.1c03001.

[18] M. Zeppilli, E. Dell'Armi, M.P. Papini, M. Majone, Sequential reductive/oxidative bioelectrochemical process for groundwater perchloroethylene removal, Chem. Eng. Trans. 86 (2021) 373−378, https://doi.org/10.3303/CET2186063.

[19] F. Aulenta, L. Tocca, R. Verdini, P. Reale, M. Majone, Dechlorination of trichloroethene in a continuous-flow bioelectrochemical reactor: effect of cathode potential on rate, selectivity, and electron transfer mechanisms, Environ. Sci. Technol. 45 (2011) 8444−8451, https://doi.org/10.1021/es202262y.

[20] D. Fernández-Verdejo, P. Cortés, A. Guisasola, P. Blánquez, E. Marco-Urrea, Bioelectrochemically-assisted degradation of chloroform by a co-culture of Dehalobacter and Dehalobacterium, Environ. Sci. Ecotechnology. 12 (2022) 100199, https://doi.org/10.1016/J.ESE.2022.100199.

[21] X. Wang, F. Aulenta, S. Puig, A. Esteve-Núñez, Y. He, Y. Mu, K. Rabaey, Microbial electrochemistry for bioremediation, Environ. Sci. Ecotechnology. 1 (2020) 100013, https://doi.org/10.1016/j.ese.2020.100013.

[22] C. Cruz Viggi, M. Tucci, M. Resitano, S. Crognale, M.L. Di Franca, S. Rossetti, F. Aulenta, Coupling of bioelectrochemical toluene oxidation and trichloroethene reductive dechlorination for single-stage treatment of groundwater containing multiple contaminants, Environ. Sci. Ecotechnology. 11 (2022) 100171, https://doi.org/10.1016/j.ese.2022.100171.

[23] A. Lai, F. Aulenta, M. Mingazzini, M.T. Palumbo, M.P. Papini, R. Verdini, M. Majone, Bioelectrochemical approach for reductive and oxidative dechlorination of chlorinated aliphatic hydrocarbons, Chemosphere 169 (2017) 351−360, https://doi.org/10.1016/j.chemosphere.2016.11.072.

[24] M. Zeppilli, B. Matturro, E. Dell'Armi, L. Cristiani, M.P. Papini, S. Rossetti, M. Majone, Reductive/oxidative sequential bioelectrochemical process for Perchloroethylene (PCE) removal: effect of the applied reductive potential and microbial community characterization, J. Environ. Chem. Eng. 9 (2021), https://doi.org/10.1016/j.jece.2020.104657.

[25] A. Lai, M.L. Astolfi, V. Bertelli, V.G. Agostinelli, M. Zeppilli, M. Majone, Chromate fate and effect in bioelectrochemical systems for remediation of chlorinated solvents, N. Biotech. 60 (2021) 27−35, https://doi.org/10.1016/j.nbt.2020.06.006.

[26] A. Lai, R. Verdini, F. Aulenta, M. Majone, Influence of nitrate and sulfate reduction in the bioelectrochemically assisted dechlorination of cis-DCE, Chemosphere 125 (2015) 147−154, https://doi.org/10.1016/j.chemosphere.2014.12.023.

[27] M. Zeppilli, E. Dell'Armi, L. Cristiani, M.P. Papini, M. Majone, Reductive/oxidative Sequential Bioelectrochemical Process for Perchloroethylene Removal, Water (Switzerland), 2019, p. 11, https://doi.org/10.3390/w11122579.

[28] F. Aulenta, A. Canosa, P. Reale, S. Rossetti, S. Panero, M. Majone, Microbial reductive dechlorination of trichloroethene to ethene with electrodes serving as electron donors without the external addition of redox mediators, Biotechnol. Bioeng. 103 (2009) 85−91, https://doi.org/10.1002/bit.22234.

[29] D.E. Fennell, J.M. Gossett, S.H. Zinder, Comparison of butyric acid, ethanol, lactic acid, and propionic acid as hydrogen donors for the reductive dechlorination of tetrachloroethene, Environ. Sci. Technol. 31 (1997) 918−926, https://doi.org/10.1021/es960756r.

[30] M.M. Lorah, L.D. Olsen, Degradation of 1,1,2,2-tetrachloroethane in a freshwater tidal wetland: field and laboratory evidence, Environ. Sci. Technol. 33 (1999) 227−234, https://doi.org/10.1021/es980503t.

[31] F. Aulenta, R. Verdini, M. Zeppilli, G. Zanaroli, F. Fava, S. Rossetti, M. Majone, Electrochemical stimulation of microbial cis-dichloroethene (cis-DCE) oxidation by an ethene-assimilating culture, N. Biotech. 30 (2013) 749−755, https://doi.org/10.1016/j.nbt.2013.04.003.

[32] E. Dell'Armi, M. Zeppilli, B. Matturro, S. Rossetti, M. Petrangeli Papini, M. Majone, Effects of the feeding solution composition on a reductive/oxidative sequential bioelectrochemical process for perchloroethylene removal, Processes 9 (2021) 405, https://doi.org/10.3390/pr9030405.

[33] E. Dell'Armi, M. Zeppilli, M.L. Di Franca, B. Matturro, V. Feigl, M. Molnár, Z. Berkl, I. N, H. Yaqoubi, S. Rossetti, M. Petrangeli Papini, M. Majone, Evaluation of a bioelectrochemical reductive/oxidative sequential process for chlorinated aliphatic hydrocarbons (CAHs) removal from a real contaminated groundwater, J. Water Proc. Eng. 49 (2022) 103101, https://doi.org/10.1016/j.jwpe.2022.103101.